ISSN 1846-6168 (Print), ISSN 1848-5588 (Online)
ID: TG-20170509132026 Preliminary communication

EVALUATION OF LIMESTONE LAYER'S EFFECT FOR UWB MICROWAVE IMAGING OF BREAST MODELS USING NEURAL NETWORK

Ahmet AYDIN, Emine AVŞAR AYDIN

Abstract: X-ray mammography is widely used for detection of breast cancer. Besides its popularity, this method did not have the potential of discriminating a tumor covered with limestone from a pure limestone mass. This might cause misdetection of some tumors covered with limestone or unnecessary surgery for a pure limestone mass. In this study, Ultra-Wide Band (UWB) signals are used for the imaging. A feed-forward artificial neural network (FF-ANN) is used to classify the mass in the breast whether it is a tumor or not by using the transmission coefficients obtained from UWB signals. A spherical tumor covered with limestone and pure limestone masses were designed and placed into the fibro-glandular layer of breast model using CST Microwave Studio Software. The radius of the masses for both cases is changed from 1 mm to 10 mm with 1 mm steps. Horn antennas were chosen to send and receive Ultra-Wide Band (UWB) signals between 2 and 18 GHz frequency range. The obtained results show that the proposed method, on the contrary of the mammogram, has the potential of discriminating the tumor covered with limestone from the pure limestone, for the mass sizes of 7, 8 and 10 mm. Consequently, the UWB microwave imaging can be used to distinguish these cases from each other.

Keywords: breast cancer; feed forward artificial neural network ((FF-ANN); limestone; microwave imaging

1 INTRODUCTION

Breast cancer is one of the major causes of female death in the world and so breast cancer detection is one of the most intriguing fields of microwave imaging. An early diagnosis of tumor presence absolutely increases the survival rate in women and gives the opportunities of getting through the problem. Therefore, timely detection and early stage treatment are important factors. There are widespread detection methods such as X-ray mammography, Magnetic Resonance Imaging (MRI), and ultrasound [1-18]. Although X-ray mammography is currently the most popular screening tool, it also has its restrictions - one of them is the high misdetection ratio, and the other one is its insufficiency to discriminate between malignant and benign tumors. All existing screening tools including X-ray mammography are expensive, uncomfortable, and incapable in terms of detection and location of the tumor [1-12]. In addition to these, existing methods cannot detect the tumor if there is limestone layer, which is caused by the milk ducts, surrounding of the tumor. It is known that chemical and physical properties tissues, including their electron density and molecular dynamics, are important for imaging and diagnosis methods [15]. Consequently, limestone effect is analyzed to investigate the radiation from the skin regarding whether there is limestone or not surrounding of the tumor. These restrictions embolden to seek for the better alternative methods. Microwave Ultra-Wide Band (UWB) imaging, which is one of the alternative methods, is the most interesting method these days [5, 10, 16-18]. In this method, the system consists of one transmitting and one receiving antenna to send and record UWB signals through the breast tissue. Microwave imaging utilizes the difference in the dielectric properties of benign and malignant breast tissues. And the previous studies show that artificial neural networks can be trained based on this difference to automate diagnosis phase [19-22].

2 BREAST DESIGN AND DATA COLLECTION

There have been alternative breast design dimensions [16-18]. We have done a hemisphere shape design as showed in Fig. 1 and Tab. 1.

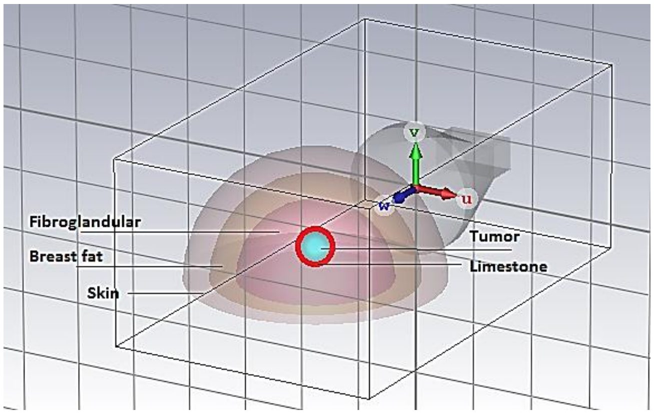

Figure 1 A simple breast model with layers

Table 1 Breast layer sizes

Model Layer	Diameter	Thickness
Skin	10 cm	2 mm
Breast fat	8 cm	2 mm
Fibro glandular	6 cm	2 mm

Table 2 Debye parameters of breast model layers at 6 GHz [23]

Tissue	ε_∞	ε_s	σ_s	τ (ps)
Skin	4.00	37.00	1.10	7.37
Breast fat	6.57	16.29	0.23	7.00
Fibro glandular	5.28	35.14	0.46	7.00
Tumor	3.99	54.00	0.70	7.23

The Debye parameters that have been used are shown in Tab. 2 [23] where, ε_∞, ε_s and τ, are exponent parameters, infinite permittivity constant, static permittivity constant, and time constant, respectively.

Tumor radius sizes have been chosen from 0.2 cm to about 1.5 cm in the literature [24-28]. However, 0.25 cm is the frequently used one. Besides, it is ideal for the minimum used tumor size. We created a spherical tumor with radius from 1mm (0.1 cm) to 10 mm (1 cm). Although dielectric properties of the healthy and fat tissues are generally constant, this case is not the same for the tumor. In other words, the dielectric property of the tumor changes with respect to the frequency. The main aim of this study is to discriminate a tumor covered with limestone from a pure limestone mass. Therefore, a spherical tumor model covered with limestone and pure spherical limestone model were designed. The used frequency range is from 2 GHz to 18 GHz in our simulation study. To obtain the data, we applied the following steps:

1) As shown in Fig. 2, lay down a pair of transmitter-receiver horn antennas at opposite sides of the breast model in the axis.
2) Put a spherical tumor model covered with limestone and pure spherical limestone model at any location l along the y-axis in the breast model.
3) Transmit signal using plane wave and receive the signal on the opposite side.
4) Transmission coefficients over the breast tissue with a spherical tumor model covered with limestone and pure spherical limestone model are obtained.
5) The above-mentioned steps are performed for 10 different radii.

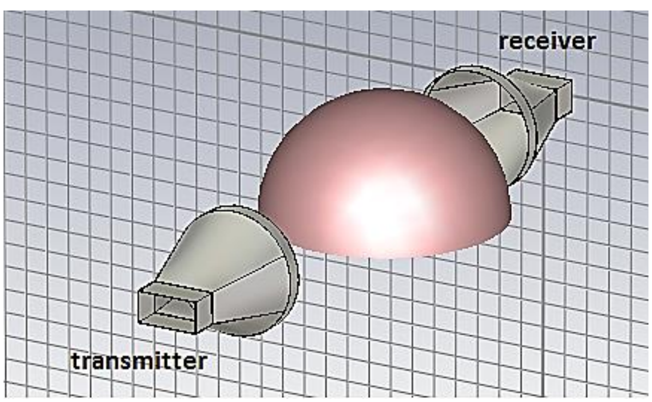

Figure 2 Measurement setup in CST Microwave Studio

Furthermore, the breast model was simulated to get the propagated signals through breast model with a spherical tumor model covered with limestone and pure spherical limestone model. The distance between transmitter and receiver antennas is only 25.9925 cm. Therefore, noise is remissible in this case.

Microwave imaging is performed by transmitting a sequence of electromagnetic waves through the female breast and measuring the scattered field on the breast. The electromagnetic signals fed to the transmitting antennas and captured by the receiving antennas are characterized by scattering parameters "S-parameters". Data acquisition process was conducted under simulation environment using CST Microwave Studio Software. The frequency was set from 2 GHz to 18 GHz. Fig. 2 shows the data collection process using Horn antennas at opposite sides of the breast model in the axis. This data process is repeated for 10 different radii of tumor.

3 TUMOR DETECTION USING ARTIFICIAL NEURAL NETWORK

One of the main problems of the mammogram is that the pure limestone and a tumor covered with limestone will produce same images on the X-ray film and this makes it impossible to distinguish these two cases from each other. However, the UWB imaging has the potential of discriminating these two cases from each other.

In this study, a feed-forward artificial neural network (FF-ANN) is trained to classify and predict the situation of the mass in the breast and decide whether it is a tumor covered with limestone or only a limestone without tumor. The input of the FF-ANN is the measurement frequency and the transmission coefficient parameters obtained at the receiver antenna, and the output is the classification result as a tumor or not. The transmission coefficients of the simulation result are given as complex numbers. The magnitude of these complex numbers is used for the FF-ANN. Although the simulation data is obtained for the frequencies between 2 ÷ 18 GHz, the data between 6.48 ÷ 11.50 GHz is more separable. Hence, the data between these frequencies, totally 315 different samples for each case, is used. The mean, range, standard deviation of the input data and the correlation between the data of the tumor covered with limestone and pure limestone are given in Table 3 for each mass size.

Table 3 Mean, range and standard deviation of the input data for each mass size

Mass Size (mm)	Mean	Range	Standard Deviation	Correlation
1	0.0271	0.0191	0.0056	0.9999
2	0.0270	0.0194	0.0056	0.9998
3	0.0271	0.0189	0.0055	1.0000
4	0.0271	0.0191	0.0056	0.9999
5	0.0270	0.0189	0.0055	0.9998
6	0.0271	0.0188	0.0055	0.9999
7	0.0274	0.0201	0.0055	0.9859
8	0.0263	0.0196	0.0054	0.9882
9	0.0296	0.0208	0.0060	0.9798
10	0.0293	0.0231	0.0064	0.9699

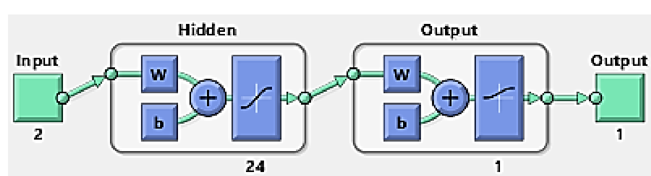

Figure 3 The ANN model schematic

For the number of the nodes in the hidden layer, all cases between 5 ÷ 25 nodes are tested and the best results are obtained with 24 nodes, Fig. 3. The learning function is selected as scaled conjugate gradient (trainscg) in MATLAB.

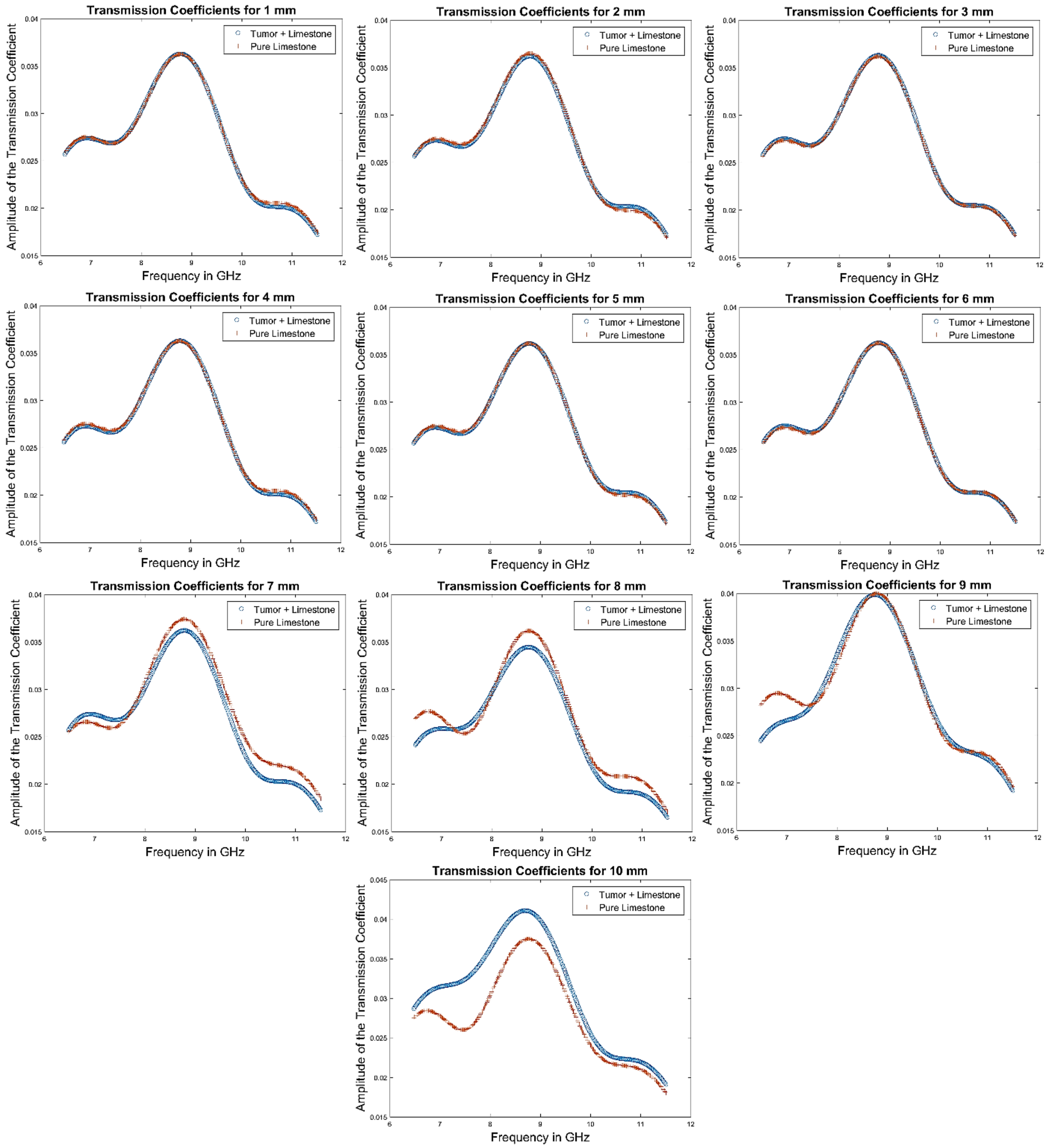

Figure 4 The transmission coefficients of tumor covered with limestone and pure limestone for mass sizes between 1 ÷ 10 mm

4 RESULTS AND DISCUSSIONS

10-fold cross validation is used to train and test the FF-ANN model. The data folds are created by randomly sampling the input data into 10 different groups. 9 groups are used for training and the last one for testing. These steps are repeated for all folds and the mean of the Correct Rate, Sensitivity and Specificity are calculated as total performance metric. The obtained results for different mass sizes are given in Tab. 4.

The prediction results, which are given in Tab. 4, show that the proposed method, on the contrary of the mammogram, has the potential of discriminating the tumor covered with limestone from the pure limestone, for the mass sizes of 7, 8 and 10 mm.

The reason why the method did not work well for the other mass sizes is that there is no usable difference between transmission coefficient parameters at any frequency in the given range, as it can be seen in Fig. 4 and Tab. 3.

Table 4 Mean Correct Rate, Sensitivity and Specificity for 10-fold cross validation of each mass size

Mass Size (mm)	Correct Rate	Sensitivity	Specificity
1	0.4889	0.4177	0.5680
2	0.4778	0.5022	0.4458
3	0.4841	0.4757	0.5263
4	0.4968	0.4845	0.5205
5	0.4905	0.4488	0.5565
6	0.4460	0.4857	0.4071
7	0.9111	0.8992	0.9249
8	0.8667	0.8167	0.9217
9	0.5524	0.5963	0.5303
10	0.9968	1.0000	0.9943

As a result of this study, if the examined mass size is 7,8 or 10 mm, the trained FF-ANN can be used for any input frequency and resultant transmission coefficient parameters between 6.48 ÷ 11.50 GHz to predict whether the mass is a tumor covered with limestone or pure limestone.

5 CONCLUSION

The results of the study show that UWB microwave imaging outperforms X-ray mammogram in cases of discriminating a tumor covered with limestone from a pure limestone mass. Although the UWB microwave imaging is a promising method for the mentioned problem, the performance of the method for the mass sizes smaller than 7 mm can be increased with different antenna designs. Therefore, better transmission coefficients, which make it possible to differentiate both cases from each other, might be obtained.

6 ACKNOWLEDGEMENT

This article is supported by the Scientific Research Unit of Adana Science and Technology University (Project number: 16119001).

7 REFERENCES

[1] Mahalakshmi, N.; Eyakumar, J. V.: Design and Develeopment of Single Layer Microstrip Patch Antenna for Breast Cancer Detection. // Bonfiring International Journal of Research in Communication Engineering, 2, 1(2012).

[2] Yu, J.; Yuan, M.; Liu, Q. H. A Wideband Half Oval Patch Antenna for Breast Imaging. // Progress in Electromagnetics Research, PIER 98, 2009, pp. 1-13.

[3] Saw, A.; Jone, A. A. Ultra Wide Band Radar Based Breast Cancer Detection Using Stacked Patch and Wide Slot Antenna. // International Journal of Electronics Signals and Systems, 3, (2013).

[4] Bohra, S.; Shaikh, T. UWB Microstrip Patch Antenna for Breast Cancer Detection, International Journal of Advanced Research in Electronics and Communication Engineering (IJARECE), 5, (2016).

[5] Adnan, S.; Abd-Alhameed, A.; Hraga, H. I.; Elfergani, I. T. E.; Noras, J. M.; Halliwell, R. Microstrip Antenna for Microwave Imaging Application. // Progress in Electromagnetics Research Symposium, Marrakesh, Morocco, 2011, pp. 20-23.

[6] Singh, S. K.; Singh, A. K. UWB Rectangular Ring Microstrip Antenna with Simple Capacitive Feed for Breast Cancer Detection. // Progress in Electromagnetics Research Symposium, Beijing, China, 2009, pp. 23-27.

[7] Choudhary, H.; Choudhary, R.; Vats, A.: Design and Analysis of Circular Patch Microstrip UWB Antenna for Breast Cancer Detection. // International Journal of Innovative Research in Science Engineering and Technology (IJIRSET), 4, (2015).

[8] Minz, L.; Simonov, N.; Ik Jeon, S.; Lee, J. M. Dual Layer UWB Dielectric Probe for Bistatic Breast Cancer Detection System, Proceedings of ISAP2012, Nagoya, Japan, 2012.

[9] Ragha, L. K.; Bhatia, M. S. Numerical Assessment of UWB Patch Antenna for Breast Tumor Detection. // ACEEE Int. J. on Electrical and Power Engineering, 1, 3(2010).

[10] Bah, M. H.; Hong, J. S.; Jamro, D. A. Ground Slotted Monopole Antenna Design for Microwave Breast Cancer Detection Based on Time Reversal MUSIC. // Progress in Electromagnetics Research C, 59, (2015), pp. 117-126.

[11] Kim, T. H.; Pack, J. K.: Measurement of Electrical Characteristics of Female Breast Tissues for the Development of the Breast Cancer Detector, 30, (2012), pp. 189-199.

[12] Adnan, S.; Abd-Alhameed, R. A.; See, C. H.; Hraga, H. I.; Elfergani, I. T. E.; Zhou, D.: A Compact UWB Antenna Design for Breast Cancer Detection. Progress in Electromagnetics Research Symposium Proceedings, China, 2010, pp. 887-890.

[13] Cheng, X.; Mao, J.; Bush, R.; Kopans, D. B.; Moore, R. H.; Chorlton, M.: Breast cancer detection by mapping hemoglobin concentration and oxygen saturation. // Applied Optics, 42, 31(2003).

[14] Ovechkln, A. M.; Yoon, G. Infrared Imaging for Screening Breast Cancer Metastasis Based on Abnormal Temperature Distribution. // Journal of the Optical Society of Korea, 9, 4(2005), pp. 157-161.

[15] Emwas, A. M.; Antakly, T.; Saoudi, A.; Al-Ghamdi, S.; Serrai, H. Magnetic Resonance Spectroscopy and Imaging in Breast Cancer Prognosis and Diagnosis. // Applications of NMR Spectroscopy, 3, (2015), pp. 4-35.

[16] Shao, W.; Zhou, B. UWB microwave imaging for breast tumor detection inhomogeneous tissue. // Proceedings of the 2005 IEEE Engineering in Medicine and Biology, 27th Annual Conference, Shanghai, China, 2005, pp. 1496-1499.

[17] Fear, E. C.; Stuchly, M. A. Microwave detection of breast cancer. // IEEE Transactions on Microwave Theory and Techniques, 48, (2000), pp. 1854-1863.

[18] Klemm, M.; Craddock, I.; Leendertz, J.; Preece, A.; Benjamin, R. Experimental and clinical results of breast cancer detection using UWB microwave radar. // Proceedings of IEEE Antennas and Propagation Society International Symposium, 2008, pp. 1-4.
[19] Abdel-Zaher, A. M.; Eldeib, A. M. Breast cancer classification using deep belief networks. // Expert Systems with Applications, 46, (2016), pp. 139-144.
[20] Caorsi, S.; Lenzi, C. A Breast Cancer Detection Approach Based on Radar Data Processing using Artificial Neural Network. // Research Journal of Advanced Engineering and Science, 1, 4(2016), pp. 213-222.
[21] Guan, J. S.; Lin, L. Y.; Ji, G. L.; Lin, C. M.; Le, T. L.; Rudas, I. J. Breast Tumor Computer-aided Diagnosis using Self-Validating Cerebellar Model Neural Networks. // Acta Polytechnica Hungarica, 13, 4(2016).
[22] Żejmo, M.; Kowal, M.; Korbicz, J.; Monczak, R. Classification of breast cancer cytological specimen using convolutional neural network. // In Journal of Physics: Conference Series, 783, (2017), 012060.
[23] Khuda, I.; Khatun, S.; Reza, K. J.; Rahman, Md. M.; Fakir, Md. M. Improved debye model for experimental approximation of human breast tissue properties at 6 GHz ultra-wideband centre frequency. // International Journal of Engineering and Technology (IJET), 5, 6(2013), pp. 4708-4717.
[24] Sill, J. M.; Fear, E. C.: Tissue sensing adaptive radar for breast cancer detection-experimental investigation of simple tumor models. // IEEE Transactions on Microwave Theory and Techniques, 53, (2005), pp. 3312-3319.
[25] Wang, M.; Yang, S.; Wu, S.; Luo, S. A RBFNN approach for DoA estimation of ultra-wideband antenna array. // Neurocomputing, 71, (2008), pp. 631-640.
[26] Lim, H. B.; Nhung, N. T.; Li, E.; Thang, N. D. Confocal microwave imaging for breast cancer detection: Delay-multiplyand-sum image reconstruction algorithm. // IEEE Transactions on Biomedical Engineering, 55, (2008), pp. 1697-1704.
[27] Fear, E. C.; Still, J.; Stuchly, M. A. Experimental feasibility study of confocal microwave imaging for breast tumor detection. // IEEE Transactions on Microwave Theory and Techniques, 51, (2003), pp. 887-897.
[28] Davis, S. K.; Tandradinata, H.; Hagness, S. C.; Veen B. D. Ultra-wideband microwave breast cancer detection: A detection-theoretic approach using the generalized likelihood ratio test. IEEE Transactions on Biomedical Engineering, 52, 7(2005), pp. 1237-1250.

Authors' contacts:

Ahmet AYDIN, Assistant Prof. Dr.
Çukurova University,
Department of Biomedical Engineering
Sarıçam-Adana/TURKEY
aaydin@cu.edu.tr

Emine AVŞAR AYDIN, Assistant Prof. Dr.
Adana Science and Technology University,
Department of Aeronautics Engineering
Adana/TURKEY
eaydin@adanabtu.edu.tr
rasvaenime@gmail.com